Nonadiabatic response to short intense laser pulses in dissociation dynamics

R. Numico, A. Keller, and O. Atabek
Laboratoire de Photophysique Moléculaire du CNRS, Bâtiment 213, Université Paris Sud, Campus d'Orsay, 91405 Orsay, France
(Received 11 July 1996)

Molecular nonadiabatic response to the sudden switching on (rise times of few femtoseconds) of intense (tens of TW/cm^2) laser pulses may lead to some unexpected enhancements of dissociation rates. These effects are accounted for by the spreading of the molecule-plus-field wave packet over several resonances (instead of a single one predicted when the laser is adiabatically switched on) interfering during the excitation process. Typical time-resolved signatures of such highly nonlinear responses are thoroughly investigated in terms of the evolution of vibrational survival probabilities and fragment kinetic energy spectra of H_2^+ molecular ion taken as an illustrative example. A plausible 532-nm wavelength single-photon dissociation scenario bringing into the system less energy than the minimum required for the fragmentation to occur is examined. The suggested mechanism, which may be termed below-threshold dissociation, as opposed to above-threshold dissociation, refers to a very sharp rise of the laser pulse resulting into temporal excitation of some resonances lying above the single-photon dissociation energy, with efficient decay rates. [S1050-2947(97)09907-1]

PACS number(s): 42.50.Hz, 33.80.Gj, 33.80.Wz

I. INTRODUCTION

Recent advances in laser technology have drawn renewed interest in the study of multiphoton phenomena in atomic and molecular physics. Especially in the range of very intense and sharp fields, nonperturbative mechanisms have to be considered for the theoretical description of the fragmentation process [1,2].

In order to dissociate, a stable molecule has to absorb a certain amount of energy. The initial *excitation* step proceeds along different pathways depending on the energy deposit: from a single but energetic photon to an accumulation of a high number of photons each carrying a tiny dose of collisional energy. In the visible or UV wavelength domain, in general, a single photon brings enough energy to excite a valence electron leading to dissociation, as opposed to the IR wavelength domain where several photons may be necessary for the breaking of the chemical bond. In intense fields, an interesting theoretical prediction [3] that has experimentally been confirmed [4] is the possibility for the molecule to continue on absorbing photons even when a single-photon excitation (on purely energetic grounds) is enough for the fragmentation to occur. This phenomenon, in connection with similar behaviors in atoms [i.e., above-threshold ionization (ATI)] [5], has been termed above threshold dissociation (ATD) [3,4]. The experimental fingerprints of ATD consist in equally spaced (by the photon frequency) multiple peaks in absorption spectra [4]. The very high intensity of the field is one of the relevant parameters governing such energy accumulation in the excitation step. But still another parameter is the steepness of the rise and fall of the laser pulse rather than its magnitude. Referring to sharp laser pulses, the conditions for the validity of the adiabatic theorem are no longer fulfilled [6,7]; an initial state is distributed over quasi-stationary resonance states, continuously connected to higher excited states of the static system, which then decay into ATD channels producing highly energetic photofragments.

The subsequent *fragmentation* step displays the different energy redistribution scenarios between the modes of the molecule-plus-field system, carrying information on the cumulative history of the overall dynamics. Unexpected abundances of photofragments with low kinetic energy or even the suppression of the dissociation in very strong fields are among the possible issues of nonlinear multiphoton dynamics. The so-called bond softening or hardening mechanisms [8–12], according to which the laser may alter the molecule-plus-laser system external force fields either by lowering some potential barriers or by creating quasi-stable structures, are invoked to interpret the observations. Molecular alignment involving rotational enegy redistribution [13], high-order harmonic generation [14], and even Coulomb explosion [15] resulting from the interplay of ionization and dissociation, are other reaction pathways in competition.

In this work the ATD dynamics of the simplest molecular ion H_2^+, on which there is already considerable literature [16], is reconsidered by emphasizing the nonadiabatic response, in the *excitation* step, to a very rapid rate of change of the laser pulse. The nonlinear processes arising from an intensity increase of the field, within the framework of the adiabatic theorem (adiabatic switching on of the laser), have already been thoroughly interpreted in terms of partial fluxes [17] or wave-packet populations [8] of the *fragmentation* step. Actually, our purpose is to go beyond the adiabatic frame to examine the effect of very sharp laser pulses on photofragment kinetic energy distributions, and to address the question of controlling the outcome of the fragmentation process by pulse shaping. This paper is organized as follows. Section II gives a theoretical overview of the wave-packet propagation method to calculate photofragment kinetic energy distributions. Moreover, a simple two-level system coupled to a continuum is worked out using either a smooth or a sudden switching on of the laser pulse, leading to an interpretation of the excitation step in terms of the preparation of one or more laser induced resonances. Typical signatures of nonadiabaticity on the time-dependent behaviors of survival probabilities are depicted. Section III is devoted to a detailed analysis of calculations performed on H_2^+, by referring to the two-resonance model as an interpre-

tative tool. Excitation wavelengths are taken in the range $\lambda = 80-160$ nm corresponding to the maximum of the single-photon absorption band, resulting either in bond softening (λ in the red wing) or vibrational trapping (λ in the blue wing). In both cases the predictive ability of the simple model is tested on survival probabilities by adequately adjusting the laser pulse sharpness so as to go from a smooth to a sudden switching on of the field with, as a consequence, the nonadiabatic temporal excitation of several resonances mediating the dissociation dynamics. The basic motivation remains, however, the understanding and prediction of nonadiabatic pulse shape effects on protons kinetic energy spectra. Here the laser parameters are taken close to those used for the experimental ATD spectra [4] (532-nm wavelength and 50–100 TW/cm^2 intensity). In addition to the interpretation of satellite vibrational ATD peaks they provide, the calculations also predict a somewhat unexpected molecular fragmentation process with a single photon bringing (when considered alone) less energy than the dissociation threshold. This new phenomenon resulting from nonadiabacity, which we call below-threshold dissociation (BTD), is evidenced by a very sharp laser pulse.

II. THEORY

Molecular dynamics using superintense lasers cannot be treated within the frame of perturbative methods, especially when the electric field strength becomes comparable to internal force fields associated with the Coulomb interactions between the particles of the system. In the same way, when referring to sudden changes of laser pulse shapes, the construction of the so-called Floquet states, although useful for some interpretations, may not be appropriate. The method that is actually retained is solving the Schrödinger equation as an initial value problem. The time evolution of an initial wave packet describing the (v,J) rovibrational state of H_2^+, on the two electronic states $(1s\sigma_g,v,J)^2\Sigma_g^+$ and $(2p\sigma_u)^2\Sigma_u^+$, which, in the Born-Oppenheimer approximation account for the dissociation process

$$H_2^+(1s\sigma_g)+n\hbar\omega \rightarrow H_2^+(2p\sigma_u)\rightarrow H^+ + H(1s), \quad (1)$$

is governed by

$$i\hbar \frac{d}{dt}\begin{pmatrix}\Psi_g(R;t)\\ \Psi_u(R;t)\end{pmatrix} = \mathbf{H}(t)\begin{pmatrix}\Psi_g(R;t)\\ \Psi_u(R;t)\end{pmatrix}, \quad (2)$$

where Ψ_g and Ψ_u are the wave-packet components on the ground g and excited u states, respectively. R designates the nuclear coordinate. The Hamiltonian is written as

$$\mathbf{H(t)} = \begin{pmatrix} -\frac{\hbar^2}{2m}\frac{d^2}{dR^2}+V_g(R) & -\mu(R)\mathcal{E}(t) \\ -\mu(R)\mathcal{E}(t) & -\frac{\hbar^2}{2m}\frac{d^2}{dR^2}+V_u(R)\end{pmatrix}. \quad (3)$$

m is the reduced mass, $V_g(R)$ and $V_u(R)$ the potential energies, and $\mu(R)$ the electronic transition dipole moment. The electric field amplitude $\mathcal{E}(t)$ is given as the product of a shape function $f(t)$ by a cosine form with peak frequency ω:

$$\mathcal{E}(t) = f(t)\cos\omega t, \quad (4a)$$

where

$$f(t) = \begin{cases} f_0 e^{-(t-t_0)^2/\tau^2} & \text{for } t<t_0 \\ f_0 & \text{for } t_0<t<T \\ f_0 e^{-(t-t_0-T)^2/\tau^2} & \text{for } t>T. \end{cases} \quad (4b)$$

Finally, the initial field-free state is the ground rovibrational $(v=0,J=0)$ level of the g potential.

The persistance of the molecule-field coupling, a consequence of the divergence of the transition moment at infinity as $R/2$, avoids a proper scattering-type representation of uncoupled fragments. Gauge transformations are a possible way to overcome this difficulty, which is particularly relevant when using continuous wave lasers [18]. In the case of short pulses the asymptotic channels are obviously uncoupled after the pulse falls off. However, to avoid large wave-packet spreadings in the asymptotic region (defined by constant potentials, actually zero for H_2^+), we use an analytic propagation based on Volkov states [19], whereas in the inner region [where the potentials $V_g(R)$ and $V_u(R)$ are still varying with R] a standard three-point split-operator technique is adopted [20]. Protons kinetic energy spectra is then obtained as the probability $\mathcal{P}$ to detect the photofragments with a momentum ranging between k and $k+dk$:

$$\mathcal{P}(k)dk = \lim_{t\rightarrow\infty}[|\hat{\Psi}_g(k;t)|^2+|\hat{\Psi}_u(k;t)|^2], \quad (5)$$

$\hat{\Psi}_{g,u}$ being the Fourier transforms of the corresponding $\Psi_{g,u}$:

$$\hat{\Psi}_{g,u}(k;t) = \frac{1}{2\pi}\int_0^\infty dR e^{-ik\cdot R}\Psi_{g,u}(R;t). \quad (6)$$

We emphasize that the long time limit involved in Eq. (5) means not only that the laser is switched off but also that all dissociating wave-packet components (i.e., on the continuum states) have already proceeded to the far asymptotic region.

In order to provide an elementary understanding and interpretation of the adiabatic or sudden responses to the laser field, we now consider an oversimplified two-level system $|\chi_0\rangle$ and $|\chi_1\rangle$ coupled to a continuum of states $|\phi_E\rangle$ by a time-dependent interaction $I(t)$. To be more specific, we assume that $I(t)$ mimics the laser pulse shape $\epsilon(t)$ and consider flat top pulses with well-separated switch-on and switch-off periods [Eq. (4b)]. As time is increased, the field-free discrete levels $|\chi_0\rangle$ and $|\chi_1\rangle$ move into field-induced resonances $|\phi_{(v)}(I)\rangle$ depending on the interaction I taken as a functional of time and labeled by the index $v=0,1$. In a configuration-interaction picture their expansion can be written as [21]

$$|\phi_{(v)}(I)\rangle = a_{(v)0}(I)|\chi_0\rangle + a_{(v)1}(I)|\chi_1\rangle + \int dE' b_{(v)E'}(I)|\phi_{E'}\rangle. \quad (7)$$

In addition to this I-parametrized stationary picture we assume that the initial $(t=0)$ wave packet is nothing but $|\chi_0\rangle$; i.e.,

$$|\psi(t=0)\rangle = |\chi_0\rangle. \quad (8)$$

Finally, dynamical survival probabilities $P_0(t)$ and $P_1(t)$ are defined as the components of the wave packet on $|\chi_0\rangle$ and $|\chi_1\rangle$:

$$P_v(t) = |\langle \chi_v|\psi(t)\rangle|^2. \quad (9)$$

The steepness of the interaction $I(t)$ controlling the time evolution of the wave packet may be analyzed within two approximations:

(i) Adiabatic approximation. In the case where the rate of change of the interaction is very slow, the solution of the Schrödinger equation may be approximated by means of an eigenfunction of the instantaneous Hamiltonian. In our model, the wave packet $|\psi(t)\rangle$ adiabatically follows a single resonance $|\phi_{(0)}(I)\rangle$, which, in field-free conditions, is nothing but the initial state $|\chi_0\rangle$. The time evolution has a simple expression involving the resonance eigenenergy $E_{(0)}$ parametrized by I:

$$|\psi(t)\rangle = \exp\left[-\frac{i}{\hbar}\int_0^t E_{(0)}\big(I(t')\big)dt'\right]|\phi_{(0)}(I)\rangle. \quad (10)$$

Neglecting the continuum contribution of Eq. (7), the survival probabilities are obtained as

$$P_v(t) = |a_{(0)v}(I)|^2 \quad (v=0,1). \quad (11)$$

The dynamical picture that arises, as the field is switched on, is a continuous merging of the initial state $|\chi_0\rangle$ into the resonance $|\phi_{(0)}\rangle$, which displays a nonzero component $(a_{(0)1}\neq 0)$ on $|\chi_1\rangle$. The consequence is an increase of P_1 (initially 0) and a proportional decrease of P_0 (initially 1) during the pulse rise. At the end of the pulse, with the falloff also being adiabatic (slow), the resonance $|\phi_{(0)}\rangle$ merges back into $|\chi_0\rangle$ and P_1 decreases to zero:

$$P_1(t\to\infty) = |\langle \chi_1|\phi_{(0)}(I=0)\rangle|^2 = |\langle \chi_1|\chi_0\rangle|^2 = 0. \quad (12)$$

As for $P_0(t\to\infty)$, the initial value cannot be reached due to dissociation:

$$P_0(t\to\infty) < 1. \quad (13)$$

Such are the typical signatures of the adiabatic regime. We note that the only difference from the well-known adiabatic theorem [6] is the presence of a leakage towards a dissociative continuum, as indicated by Eq. (13).

(ii) Sudden approximation. In the opposite case, an almost unchanged wave packet over a very short time interval (from 0 up to t_0) displays quite different expansions in eigenfunctions of the initial and final Hamiltonians, when considering the sudden change (from one steady form to another) experienced by the interaction over the same duration. The consequence is that the wave packet can no longer be described in terms of the evolution of a single resonance, but rather has to be expanded on the two resonances of the model, at the end of the switch on time t_0:

$$|\psi(t_0)\rangle = \sum_{v=0}^{1} c_v(t_0)|\phi_{(v)}(I(t_0))\rangle. \quad (14)$$

The subsequent evolution $(t>t_0)$ is, for simplicity, assumed to be adiabatic:

$$|\psi(t)\rangle = \sum_{v=0}^{1} c_v(t)|\phi_{(v)}(I)\rangle \quad (15a)$$

with

$$c_v(t) = c_v(t_0)\exp\left[-\frac{i}{\hbar}\int_{t_0}^{t} E_{(v)}\big(I(t')\big)dt'\right]. \quad (15b)$$

The survival probabilities (again neglecting the continuum contribution) display a much more complex behavior, involving, in addition to the sum of the squares of the expansion coefficients on each resonance, an interference term:

$$P_v(t>t_0) \simeq \sum_{i=0}^{1} |c_i(t)a_{(i)v}(I)|^2 + 2\,\mathrm{Re}\,[c_0(t)c_1^*(t)a_{(0)v}(I)a_{(1)v}^*(I)] \quad (16)$$

given by the real part (Re) of the last product of the right-hand side. Using Eq. 15(b), the interference term is shown to oscillate with a frequency w_R related to the energy differences of the two resonances, more precisely, as

$$\cos w_R t \sim \cos\left(\frac{1}{\hbar}\int_{t_0}^{t}\{E_{(0)}\big(I(t')\big) - E_{(1)}\big(I(t')\big)\}dt'\right). \quad (17)$$

The signatures, in terms of survival probabilities, of the nonadiabatic regime are quite different from those of the aforementioned adiabatic one. As the pulse rises, the two resonances are simultaneously excited, P_1 increases and P_0 decreases proportionally. During the plateau regime of the pulse P_0 and P_1 display in-phase oscillations following Eq. (17). At the end of the pulse, part of the population of $|\phi_{(1)}\rangle$ remains on $|\chi_1\rangle$, such that P_1 does not return back to its initial zero value:

$$P_1(t\to\infty) = \left|\left\langle \chi_1\middle|\sum_{v=0}^{1} c_v(t\to\infty)\phi_{(v)}(I=0)\right\rangle\right|^2 = |c_1(t\to\infty)|^2. \quad (18)$$

P_0, as previously, can no longer recover its initial value, part of the population being transferred to the dissociation continuum.

In summary, completely different dynamics hold in adiabatic or sudden regimes as the dissociation proceeds through one or several resonances. The evolution of survival probabilities we have so far analyzed give time-resolved informa-

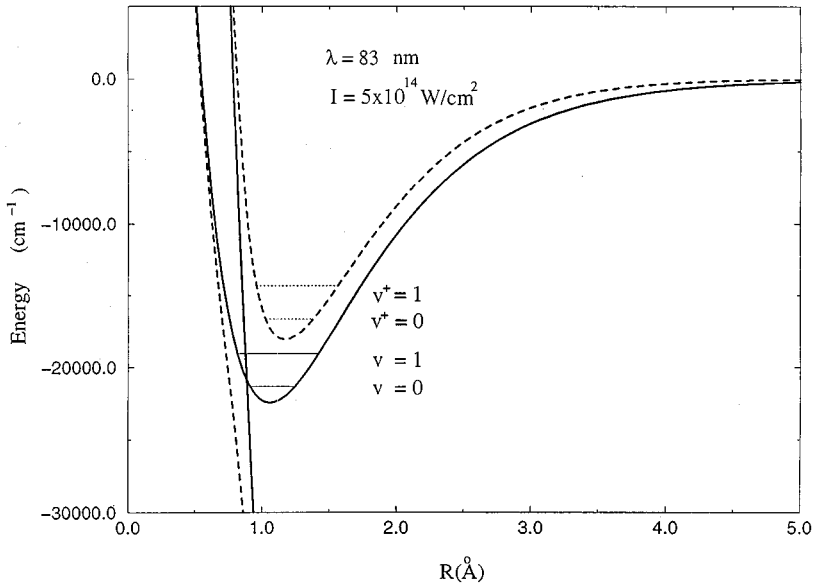

FIG. 1. Diabatic (solid line) and adiabatic (dotted line) potential energy curves of H_2^+ ground and first excited states dressed by a photon of $\lambda = 83$ nm wavelength and a laser intensity of $I = 5 \times 10^{14}$ W/cm^2.

tion on the excitation step. The observables that contain the cumulative information of the dissociation process as a whole are the kinetic energy spectra of the photofragments [Eq. (5)]. Their modification when passing from one regime to the other and the way in which fragments kinetic energies can be controlled by the laser pulse shape are the topics of the following part of the paper.

III. RESULTS

The results of quantum calculations performed on H_2^+ that are presented hereafter and interpreted in terms of the simple two-level–one-continuum model, concern two observables, namely, (i) the dynamical behaviors of survival probabilities and the total dissociation rates when referring to vibrational trapping or bond softening mechanisms by appropriately changing the nonresonant ATD laser wavelength; (ii) the protons kinetic energy distributions for the 532-nm wavelength corresponding to a multiphoton bond softening mechanism.

A. Total dissociation rates and survival probabilities

In this paragraph, three types of effects are sketched, resulting from the variation of the following laser characteristics: pulse rise time, wavelength, and intensity. The pulse *rise time* for a given intensity and wavelength is the leading parameter showing the progressive modifications from the adiabatic to the nonadiabatic responses of the molecule to the laser. Besides this, typical nonadiabatic behaviors, with respect to in-phase oscillation periods and amplitudes of survival probabilities, depend upon the variations of the *wavelength* or the *intensity* of the laser for a given pulse shape.

A first series of calculations concern a trapping mechanism resulting from the excitation of H_2^+ initially in its ground vibrational level $v = 0$ by a pulsed laser of $\lambda = 83$ nm wavelength and peak intensity of $I = 5 \times 10^{14}$ W/cm^2. The field dressed molecular potentials are displayed in Fig. 1, in both the diabatic and adiabatic frames (the latter being obtained by diagonalizing the radiative coupling). The vibrational levels are denoted $v = 0,1$ for the diabatic and $v^+ = 0,1$ for the adiabatic potentials corresponding to the maximum of the radiative coupling and their energies are indicated in the figure. The stabilization mechanism is in relation with the possibility for an initial wave packet $\chi_{v=0}$ to be trapped by the upper close adiabatic channel, which for intense fields is only weakly coupled (through kinetic terms) to the lower continuum. In other words, the dissociation dynamics is mediated by laser-induced resonances, that are very close (at least in the inner region) to the vibrational eigenfunctions χ_v^+ ($v^+ = 0,1, \ldots$) of the upper adiabatic potential. It is precisely this observation that is taken into account when representing the survival probabilities of Figs. 2

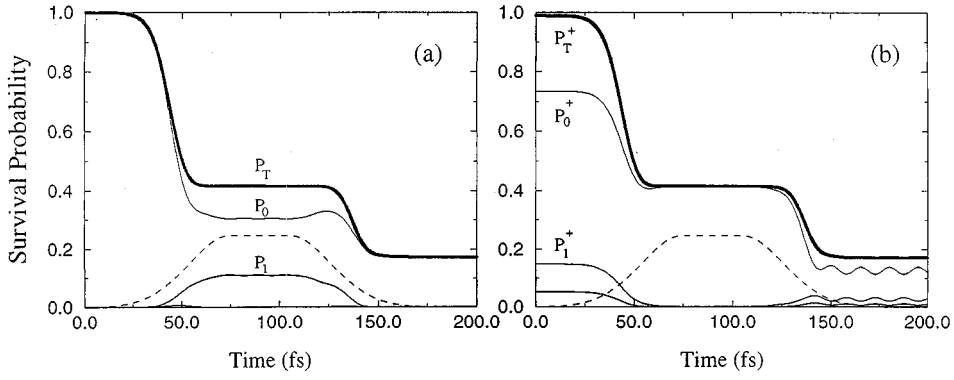

FIG. 2. Survival probabilities (solid lines) of diabatic (a) and adiabatic (b) vibrational levels for a laser pulse (arbitrary units, dashed lines) corresponding to a rise time of 40 fs. The initial field-free state is H_2^+ ($v = 0$).

and 3, in terms of the projections of the time-dependent wave packet either on the diabatic vibrational states χ_v [as in Eq. (9)] appropriate to the field-free situation, or on the adiabatic vibrational states χ_v^+, which better describe the strong radiative coupling regime. Survival probabilities that are displayed are P_0, P_1, and $P_T=P_0+P_1$ [together with their ''adiabatic'' analogues $P_v^+=|\langle\chi_v^+|\psi(t)\rangle|^2$] for three selected pulse rise times τ ranging from 40 fs (characterizing a typical adiabatic response) to 10 fs and 5 fs (inducing nonadiabatic responses). When the field is slowly switched on [as in Figs. 2(a) and 2(b)], the initial field free state $|\chi_0\rangle$ adiabatically moves into the $|\phi_{(0)}(I)\rangle$ resonance, which, during the plateau regime of the pulse, is temporarily trapped in the upper adiabatic channel and actually is accurately represented by the $|\chi_0^+\rangle$ level. This is clearly evidenced on Fig. 2(b) where P_1^+ is almost zero and $P_T^+=P_0^+$ during the pulse maximum. In the diabatic frame [Fig. 2(a)], P_1 is temporarily populated due to the fact that $|\phi_{(0)}(I_{\max})\rangle\simeq|\chi_0^+\rangle$ develops a nonzero component on $|\chi_1\rangle$. After the pulse is over, the resonance $|\phi_{(0)}(I)\rangle$ returns back to the field-free state $|\chi_0\rangle$, and P_1 recovers its initial null value, as expected when dynamics proceeds through single resonance excitation. The adiabatic frame, without physical significance in this situation, indicates only that the $|\chi_0\rangle$ state can always be expanded on the basis set of $|\chi_v^+\rangle$ adiabatic states ($v^+=0,1$ bearing the major contribution) leading to nonzero values of P_0^+ and P_1^+; their oscillations are merely related to phase accumulation during the pulse plateau. The results for a shorter pulse rise time ($\tau=10$ fs) leading to nonadiabatic behaviors are depicted in Figs. 3(a) and 3(b), namely, in-phase oscillations of P_0 and P_1 during the pulse maximum and population, which remains on P_1 after the pulse is over. In the adiabatic frame, one observes small differences between P_T^+ and P_0^+ and a rise of P_1^+ (although not very readable at that scale). These are the expected signatures of two-resonance dynamics. Much sharper pulses ($\tau=5$ fs) lead to even more complicated nonadiabatic effects such as those illustrated in Figs. 3(c) and 3(d), namely, irregular oscillations on P_0 and P_1 and non-negligible population P_2 for the diabatic frame, nonzero P_1^+, P_2^+ values during the pulse maximum for the adiabatic frame. This is clearly an indication that more than two resonances are involved in the dissociation process. Incidentally, we also note that the trapping mechanism has an increasing efficiency as the pulse is sharper: higher nonadiabaticity has as a consequence the excitation of more energetic resonances, which are better trapped in the upper closed adiabatic potentials (in terms of high-lying χ_v^+'s). The final total survival probability increases from $P_T(t_\infty)=0.2$ for $\tau=40$ fs to $P_T(t_\infty)=0.6$ for $\tau=10$ fs to reach $P_T(t_\infty)=0.9$ for $\tau=5$ fs. It is worthwhile pointing out that the excitation of several resonances during the preparation step is actually not in relation with the bandwidth of the laser, as one could imagine when referring to short pulses. Although this spreading has to be taken into account in some cases, it is rather a dynamical nonadiabatic response in relation with the sharpness of the pulse that is the leading mechanism. The argument is that two flat-topped pulses with the same plateau duration (T), having thus the same bandwidth (basically controlled by T), but different sharpnesses (different rise times τ), lead to completely different behaviors in terms of survival probabilities. Figure 4(a) displays two such pulses, with $\lambda=83$ nm, $I=5\times10^{14}$ W/cm^2, and $T=300$ fs, differing by their rise times $\tau_1=40$ fs and $\tau_2=10$ fs. Their almost equal frequency spreadings (about 100 cm^{-1}) depicted on the Fourier transforms of the pulse shapes [Fig. 4(b)], are far from the energy separation of the laser-induced resonances (about 2000 cm^{-1}). In Fig. 4(c) one observes the corresponding survival probabilities: the slow rise time leads to the single resonance adiabatic signature, whereas the sharp pulse gives the typical in-phase oscillations due to the excitation of higher resonances.

A second series of calculations shows the predictive ability of our simple model when analyzing in more detail the wavelength and intensity dependence of the nonadiabatic response. The wavelength variation (for the same initial level $v=0$, laser peak intensity $I=5\times10^{14}$ W/cm^2, and sudden pulse rise time $\tau=10$ fs) from $\lambda=83$ nm to $\lambda=105$ nm induces drastic variations in the dissociation cross section:

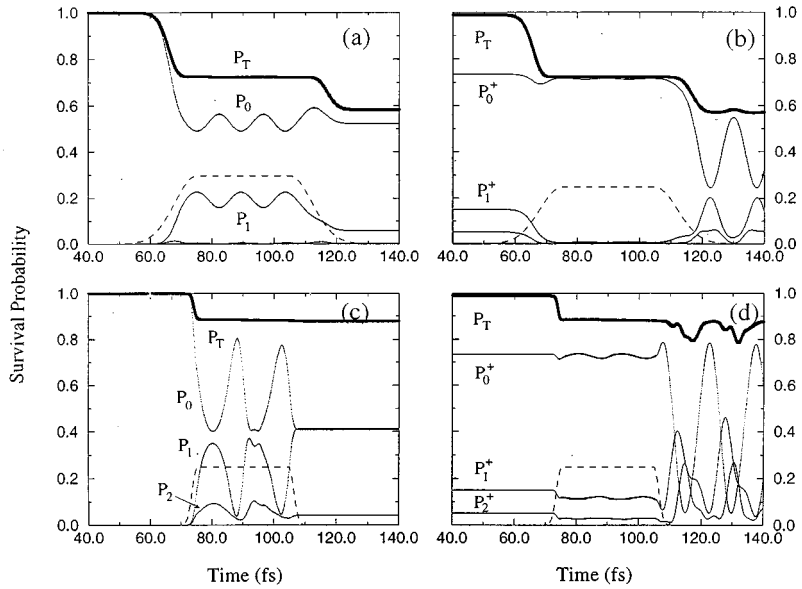

FIG. 3. Same as for Fig. 2 but with pulse rise times of 10 fs (a) and (b) and 5 fs (c) and (d).

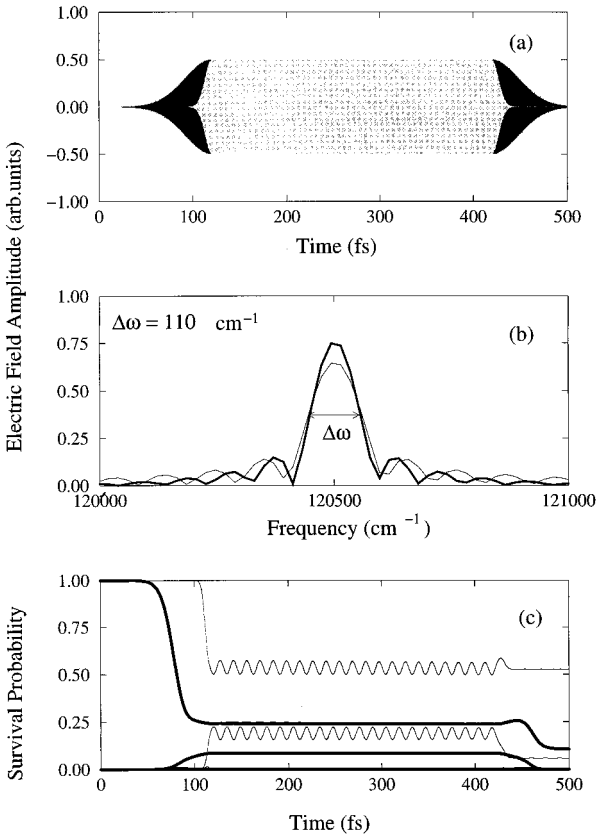

FIG. 4. Electric field amplitudes as a function of time (a) and as a function of frequency (b), and (c) the corresponding survival probabilities for two different flat-topped laser pulses with $\lambda=83$ nm wavelength, $T=300$ fs plateau duration, and $I=5\times10^{14}$ W/cm^2 maximum intensity. The thick solid line is for a slow rise time (40 fs). The thin solid line is for a fast rise time (10 fs).

from the previously analyzed stabilization situation where the total dissociation probability is 0.4 to a nearly complete dissociation with probability 0.92. The dressed molecular potentials for these two wavelengths are depicted in Fig. 5(a). The leading dissociation mechanism changes from the above-mentioned vibrational trapping for the left curve crossing at $\lambda=83$ nm to the so-called bond softening for the near maximum absorption at $\lambda=105$ nm. Figures 5(b) and 5(c) compare the time-dependent behaviors of survival probabilities for the two wavelengths. Although in completely different scales (resulting from different total dissociation cross sections), the typical in-phase oscillations during the pulse plateau of basically two survival probabilities are the common fingerprints of these trapping and softening mechanisms, where the nonadiabatic response involves a two-resonance dynamics. The main difference is that for $\lambda=83$ nm P_0 and P_1 oscillates in phase, whereas for $\lambda=105$ nm, P_1 is almost constant and it is P_0 and P_2 that show the typical oscillations. An interpretation can be provided by projecting the two resonances $|\phi_{(0)}(I_{\max})\rangle\simeq|\chi_0^+\rangle$ and $|\phi_{(1)}(I_{\max})\rangle\simeq|\chi_1^+\rangle$ on the diabatic vibrational levels $|\chi_v\rangle$ $(v=0,1,2)$ of the ground electronic state. In the left crossing situation ($\lambda=83$ nm), $|\chi_0^+\rangle$ and $|\chi_1^+\rangle$ lie close to $|\chi_0\rangle$ and $|\chi_1\rangle$, respectively, such that

$$|\phi_{(0)}(I_{\max})\rangle\propto 1|\chi_0\rangle+\epsilon|\chi_1\rangle+\epsilon^2|\chi_2\rangle, \tag{19a}$$

$$|\phi_{(1)}(I_{\max})\rangle\propto \epsilon|\chi_0\rangle+1|\chi_1\rangle+\epsilon^2|\chi_2\rangle, \tag{19b}$$

where $1,\epsilon,\epsilon^2$ are just some ordering factors. In the case where $\lambda=105$ nm, the curvature of the upper adiabatic curve is much different from the diabatic one, with, as a consequence, the lowest adiabatic level $|\chi_0^+\rangle$ lying between $|\chi_0\rangle$ and $|\chi_1\rangle$ and the second $|\chi_1^+\rangle$ close to $|\chi_2\rangle$, such that

$$|\phi_{(0)}(I_{\max})\rangle\propto 1|\chi_0\rangle+1|\chi_1\rangle+\epsilon|\chi_2\rangle, \tag{20a}$$

$$|\phi_{(1)}(I_{\max})\rangle\propto \epsilon|\chi_0\rangle+\epsilon^2|\chi_1\rangle+1|\chi_2\rangle. \tag{20b}$$

Using Eq. (16) one finally gets for $\lambda=83$ nm

$$P_0(t)\propto 1|c_0|^2+\epsilon^2|c_1|^2+2\epsilon c_0c_1\cos w_Rt, \tag{21a}$$

$$P_1(t)\propto \epsilon^2|c_0|^2+1|c_1|^2+2\epsilon c_0c_1\cos w_Rt, \tag{21b}$$

$$P_2(t)\propto \epsilon^4|c_0|^2+\epsilon^4|c_1|^2+2\epsilon^4c_0c_1\cos w_Rt, \tag{21c}$$

showing that P_0 and P_1 are oscillating with comparable amplitudes (ϵ) whereas P_2 is negligible (ϵ^4). As for $\lambda=105$ nm one has

$$P_0(t)\propto 1|c_0|^2+\epsilon^2|c_1|^2+2\epsilon c_0c_1\cos w_Rt, \tag{22a}$$

$$P_1(t)\propto 1|c_0|^2+\epsilon^4|c_1|^2+2\epsilon^2c_0c_1\cos w_Rt, \tag{22b}$$

$$P_2(t)\propto \epsilon^2|c_0|^2+1|c_1|^2+2\epsilon c_0c_1\cos w_Rt, \tag{22c}$$

with P_0 and P_2 with comparable oscillation amplitudes (ϵ) whereas P_1 is almost flat (ϵ^2).

Longer wavelengths lead to right crossing situations where the bond softening mechanism is responsible for dissociation. The calculations that are illustrated in Fig. 6 concern one of these wavelengths ($\lambda=154$ nm) and put the emphasis on the oscillation periods of the nonadiabatic survival probabilities by varying the laser peak intensity for the same pulse rise time ($\tau=5$ fs), with the initial molecular state being, as previously, the ground vibrational level $v=0$. The field dressed potentials displayed in Fig. 6(a) have a c^+ type of crossing point between the right turning points of the $v=0$ and $v=1$ vibrational levels, such that an increase of the radiative coupling strength results in an increase of the energy separation between the corresponding resonances; $E_{(0)}$ being pushed down and $E_{(1)}$ pushed up. The nonadiabatic response as a function of the laser intensity is shown in Figs. 6(b) and 6(e), in terms of the oscillation periods of the survival probability $P_1(t)$ following the prediction of Eq. (17). Namely, an increase of the peak intensity from $I=10^{12}$ W/cm^2 to $I=2\times10^{13}$ W/cm^2 results in a decrease of the oscillation period from 14.89 to 12.56 fs. This is in agreement, within 5% accuracy, with Eq. (17) where the resonance energies $E_{(v)}(I_{\max})$ are computed using time-independent techniques. We also note that there is also a fine structure in the time-dependent behavior of the survival probabilities that is evidenced in Fig. 6(f) [i.e., a closeup of Fig. 6(b)]. The oscillation period (0.25 fs) is twice the field carrier wave frequency as expected from the Floquet Hamiltonian.

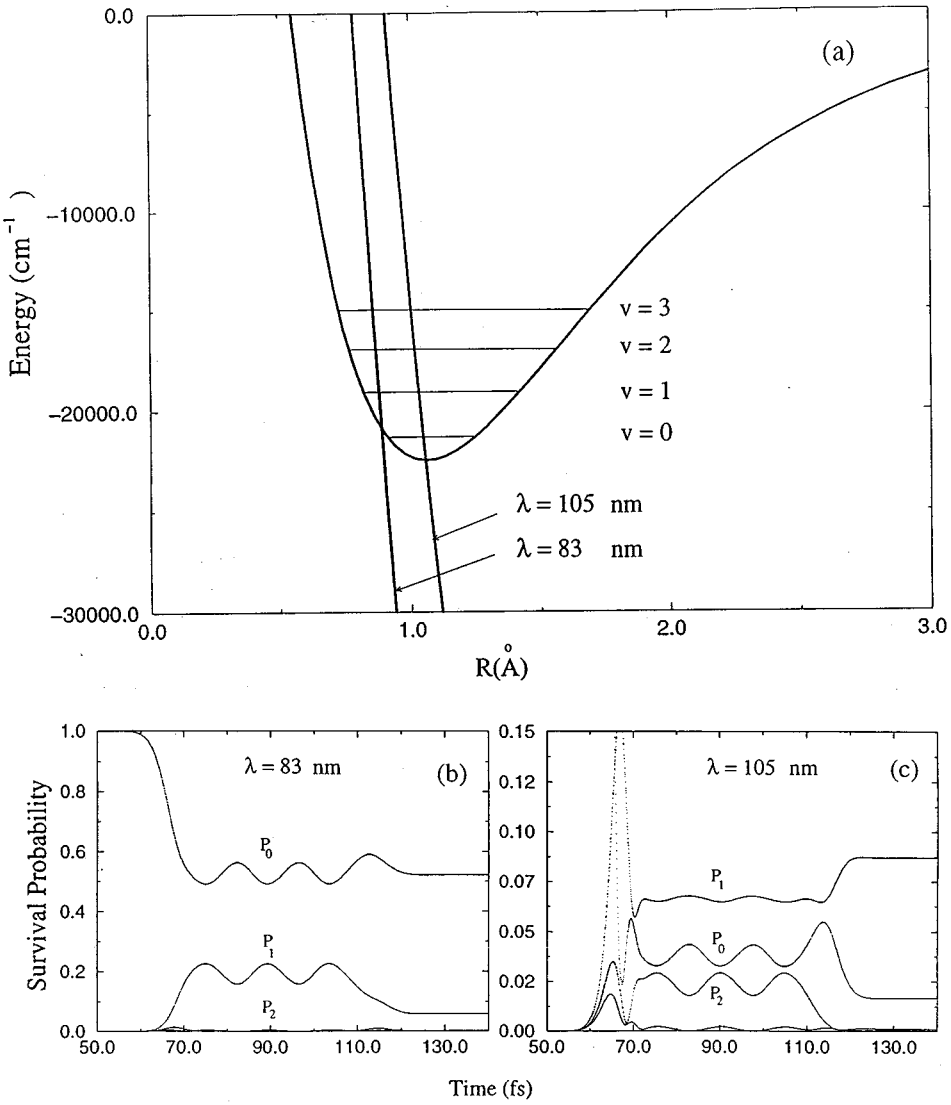

FIG. 5. (a) Vibrational energy levels and diabatic potential-energy curves of H_2^+ ground and first excited states dressed by a photon of $\lambda = 83$ nm and $\lambda = 105$ nm wavelength. (b),(c) Corresponding survival probabilities as a function of time for a laser pulse rise time of 10 fs, intensity $I = 5 \times 10^{14}$ W/cm^2, and for an initial state $v = 0$.

B. Fragments kinetic-energy spectra

We now analyze the nonadiabatic response of H_2^+ to a short intense laser pulse by considering its photofragment kinetic energy spectra. The molecule taken in an excited vibrational level $v = 2$ is supposed to be irradiated by the 532-nm harmonic of an Nd-YAG laser delivering a peak intensity of 5×10^{13} W/cm^2 as in Ref. [3]. The photon dressed molecular potentials of the two main Floquet blocks are indicated in Fig. 7. For this very nonresonant photon wavelength, although strictly speaking the $v = 2$ level shifted by the photon energy is slightly above the dissociation threshold, due to large potential barrier, the single-photon dissociation is prohibited. The dynamics proceeds via an initial absorption of 3 photons (due to favorable Franck-Condon overlap between the $v = 2$ eigenfunction of the ground electronic state g and the continuum eigenfunction of the three-photon dressed excited electronic state u). A stimulated emission takes place at $R = 2.2$ Å corresponding to a curve-crossing between the 3-photon u and the 2-photon g states; the overall mechanism is a two-photon absorption as indicated on the proton's kinetic energy spectra of Figs. 8(b) and 8(d). An adiabatically switched pulse with a rise time of $\tau = 80$ fs, providing the expected typical signature of an adiabatic response on survival probabilities (P_3, P_1 temporarily populated with a flat behavior returning back to zero after the pulse falls off, as is shown in Fig. 8(a)], results in a narrow two-photon peak [Fig. 8(b)]. A closer inspection shows a very small shoulder in the high-energy wing of this peak due to dissociation from the temporarily populated $v = 3$ level. A sharper pulse ($\tau = 20$ fs) characterizes a nonadiabatic response with the typical in-phase oscillations between P_2 and P_3 (with also a small amount of P_1) during the pulse maximum [Fig. 8(c)]. The kinetic energy spectrum [Fig. 8(d)] displays a broader two-photon peak with satellite structures displaying an energy spacing corresponding to the vibrational frequencies of $v = 0,1,2,3$ levels. Actually, the interpretation is that, during a sudden excitation, several resonances and hence several vibrational levels are simultaneously and temporarily populated, and may decay into the two-photon channel producing fragments with specific velocities. Very sharp pulses induce very strong nonadiabatic behaviors. Using rise times of $\tau = 10$ fs [Figs. 9(a) and 9(b)] or even of $\tau = 5$ fs [Figs. 9(c) and 9(d)] leads to the enhancement of the relative amplitudes of the satellite structures of the two-photon peak. But even more surprising is the rise of a one-photon peak, having in mind that a single-photon dissocia-

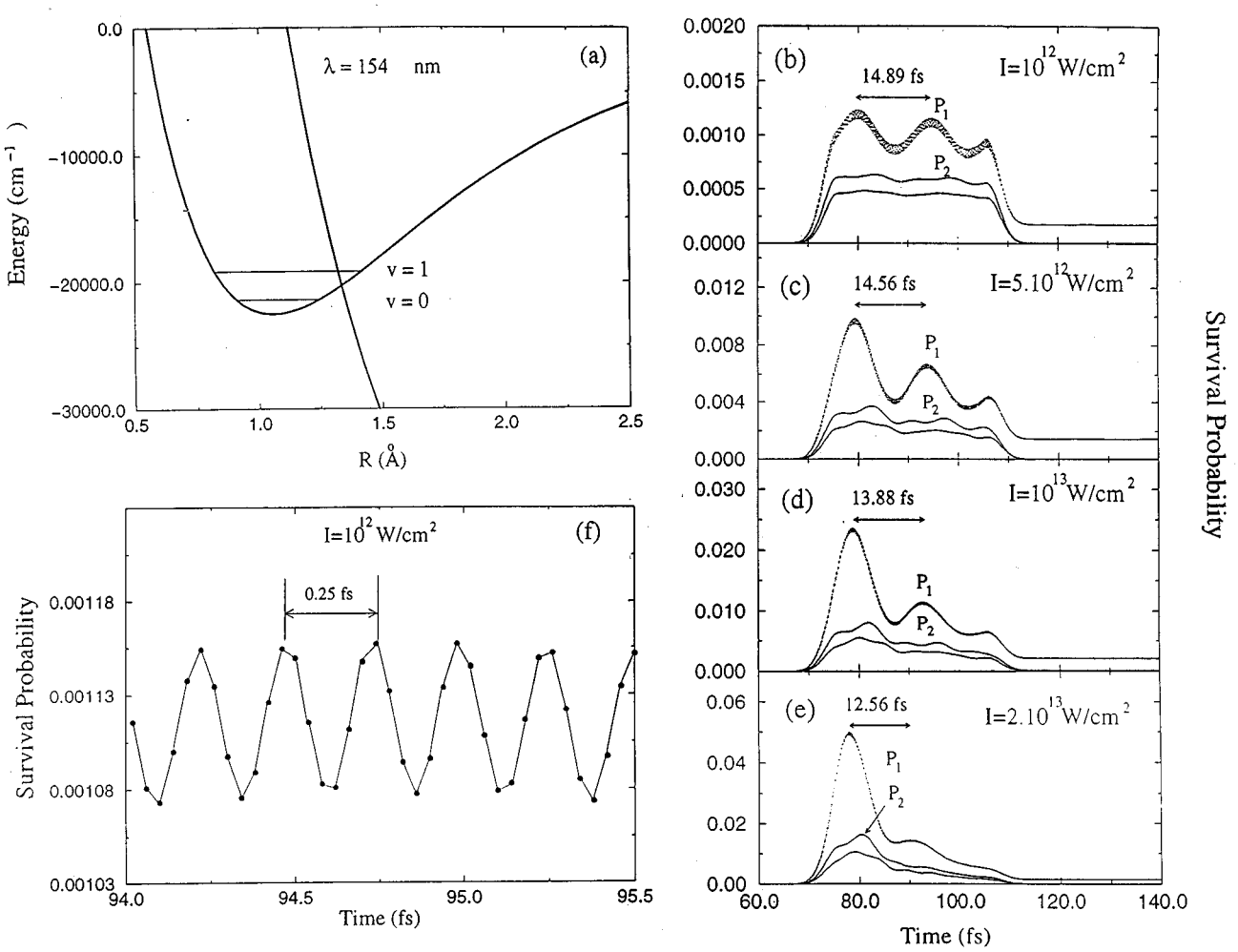

FIG. 6. (a) Potential-energy curves of the ground and first excited states of H_2^+ dressed by a photon of $\lambda = 154$ nm wavelength. (b)–(e) Corresponding survival probabilities as a function of time for a laser pulse rise time of 5 fs and increasing intensity, the initial state being $v = 0$. (f) Closeup of P_1 (b) showing the field driven fine oscillatory structure.

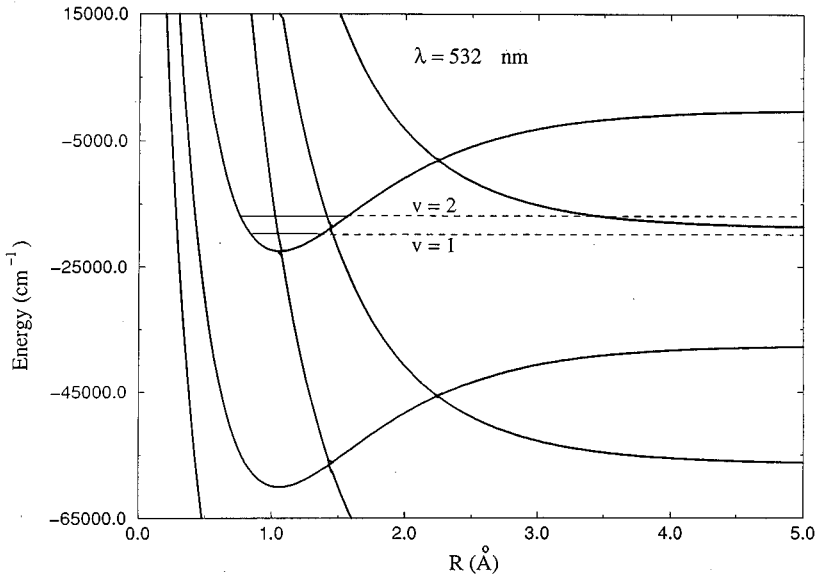

FIG. 7. Diabatic potential-energy curves for two Floquet blocks of H_2^+ dressed by a laser of $\lambda = 532$ nm wavelength.

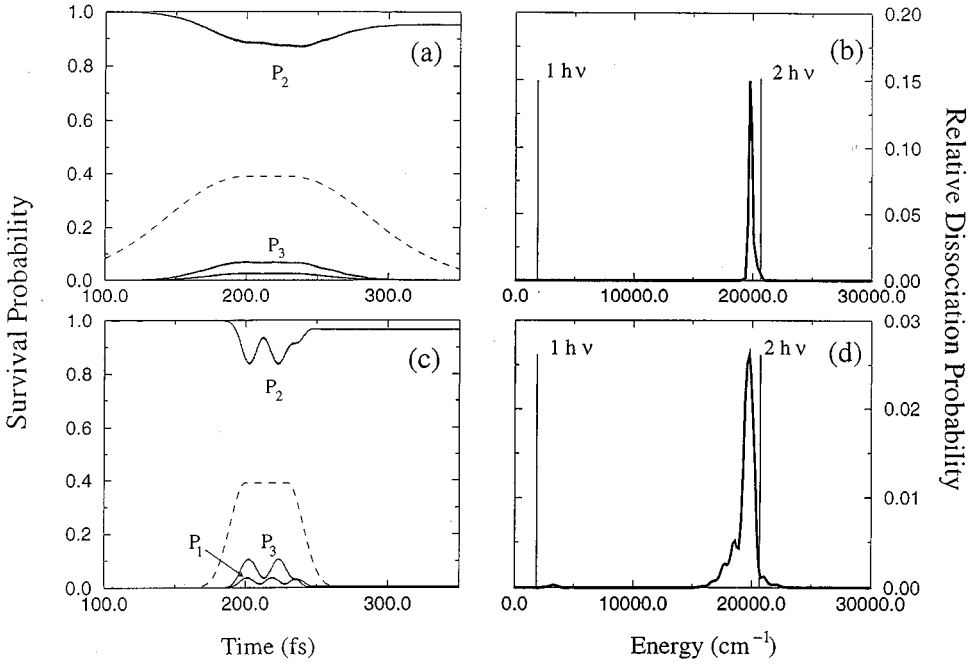

FIG. 8. (a),(c) Survival probabilities as a function of time (solid line) and laser pulse shape in arbitrary units (dashed line) for an initial state $v=2$, a 532 nm laser of intensity $I=5\times10^{13}$ W/cm^2 and two different pulse rise times of 80 fs (a) and 20 fs (c). (b),(d) Corresponding proton kinetic-energy spectra. The vertical lines indicate the energies corresponding to the absorption of 1 or 2 photons.

tion starting from $v=2$ is a very inefficient mechanism for this off-resonance wavelength. A standard bond softening mechanism by potential energy barrier lowering would necessitate a laser field more than one order of magnitude stronger.

This last observation suggests a somewhat unexpected nonadiabatic excitation scenario for dissociating a molecule with single-photon absorption, even when the energy of this photon is below the fragmentation threshold. Due to the sudden switching on of a strong field, two or more resonances with energies above the single-photon dissociation limit may be temporarily populated. It is the subsequent decay of such resonances in the one-photon channel that could be at the origin of this new phenomenon producing low-energy fragments and that we may term BTD as opposed to ATD. It is to be emphasized that the dynamics of this process is not merely related with a single resonance shifted in energy or acquiring a width large enough to be located, during the pulse, above the one-photon dissociation threshold, but is basically mediated by, at least, two laser-induced resonances. Moreover, the excitation of higher resonances responsible for BTD is not a consequence of the bandwidth of the laser pulse but, as has been shown previously (see Fig. 4, for instance), results from the sharpness of the laser pulse. In other words, the specificity of BTD is that its dynamics proceeds through some higher laser-induced resonances that do not correlate

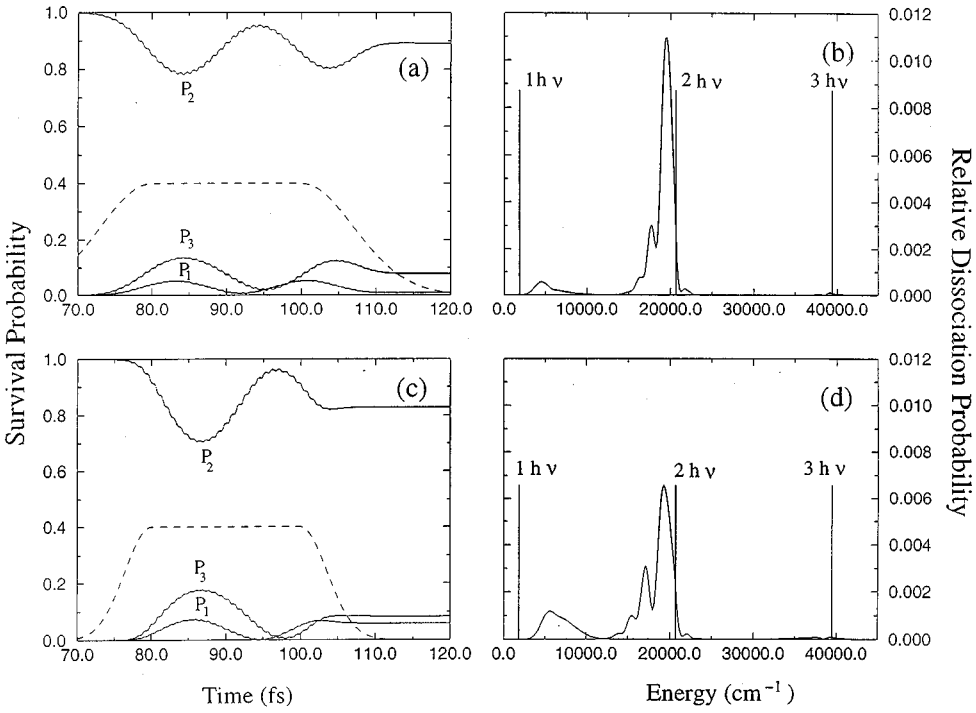

FIG. 9. Same as for Fig. 8 with pulse rise times of 10 fs for (a) and (b) and of 5 fs for (c) and (d).

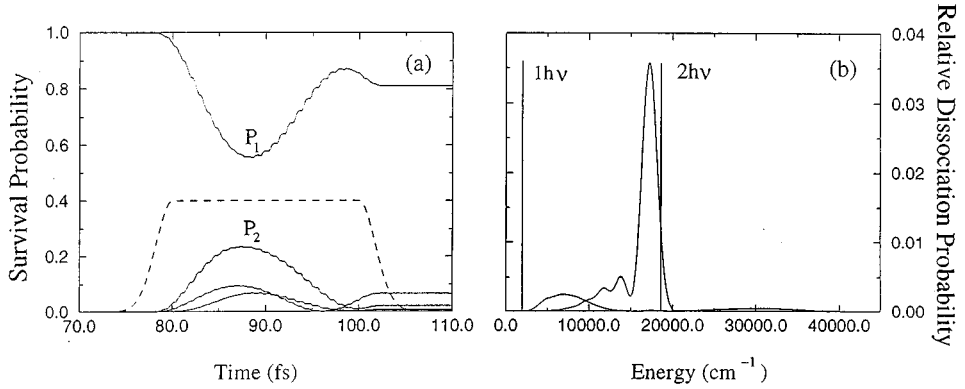

FIG. 10. Same as for Fig. 8 but for an initial state $v=1$, with a pulse rise time of 2.5 fs and intensity $I=10^{14}$ W/cm^2.

with the field-free initial state after the pulse is over. This prediction has been checked against the case of H_2^+ dissociation starting from the $v=1$ vibrational level for which the single $\lambda=532$ nm photon dissociation channel is strictly closed. Making use of a very sudden and intense laser pulse (rise time of 2.5 fs from 0 to 10^{14} W/cm^2) produces noticeable population transfer on resonances correlating with $v=2,3,\ldots$ levels carrying enough energy to decay into the one-photon channel. Figure 10 illustrates this situation with the rise of the one-photon peak.

In conclusion, the predictions of a single two-level–one-continuum model in terms of the typical signature on time-dependent survival probabilities and on the fragments kinetic energy distributions of the nonadiabatic dynamical response of a molecule to an intense laser pulse are confirmed by wave-packet calculations on H_2^+. The detailed understanding of these processes by changing laser characteristics (pulse rise time, intensity, and wavelength), encompassing the vibrational trapping and bond softening mechanisms, opens the possibility not only to control some aspects of photofragments spectra but also to evidence some single-photon dissociation mechanisms, initiated by a photon carrying less energy (when considered alone) than the minimum required for the fragmentation to occur.

ACKNOWLEDGMENTS

We acknowledge a grant of computing time on a CRAY C98 from Institut du Développement et des Ressources en Informatique Scientifique IDRIS under Project No. 940425.

[1] R. M. Potvliege and R. Shakeshaft, *Nonperturbative Treatment of Multiphoton Ionization within the Floquet Framework in Atoms in Intense Field*, edited by M. Gavrila (Academic Press, San Diego, 1992).

[2] *Coherence Phenomena in Atoms and Molecules in Laser Fields*, Vol. 28 of *NATO Advanced Studies Institute Ser. B: Physics*, edited by A. D. Bandrauk and S. C. Wallace (Plenum, New York, 1992).

[3] A. Giusti-Suzor, X. He, O. Atabek, and F. H. Mies, Phys. Rev. Lett. **64**, 515 (1990).

[4] P. H. Bucksbaum, A. Zavriyev, H. G. Muller, and D. W. Schumacher, Phys. Rev. Lett. **64**, 1883 (1990).

[5] P. Agostini, F. Fabre, G. Mainfray, G. Petite, and N. K. Rahman, Phys. Rev. Lett. **42**, 1127 (1979).

[6] T. Kato, J. Phys. Soc. Jpn. **5**, 435 (1950).

[7] K. Dietz, L. Jaeger, R. Porath, and M. Probsting, J. Chem. Phys. **102**, 7124 (1995).

[8] G. Jolicard and O. Atabek, Phys. Rev. A **46**, 5845 (1992).

[9] G. Yao and S. I. Chu, Chem. Phys. Lett. **197**, 413 (1992); Phys. Rev. A **48**, 485 (1993).

[10] A. D. Bandrauk and M. L. Sink, J. Chem. Phys. **74**, 1110 (1981).

[11] A. D. Bandrauk and G. Turcotte, J. Chem. Phys. **77**, 3867 (1982).

[12] A. Giusti-Suzor and F. H. Mies, Phys. Rev. Lett. **68**, 3869 (1992).

[13] R. Numico, A. Keller, and O. Atabek, Phys. Rev. A **52**, 1298 (1995).

[14] N. Moiseyev, M. Chrysos, R. Lefebvre, and O. Atabek, J. Phys. B **28**, 2007 (1995).

[15] S. Chelkowski, T. Zuo, O. Atabek, and A. D. Bandrauk, Phys. Rev. A **52**, 2977 (1995).

[16] For a review, see, A. Giusti-Suzor, F. H. Mies, L. F. Di Mauro, E. Charron, and B. Yang, J. Phys. B **28**, 309 (1995).

[17] M. Chrysos, O. Atabek, and R. Lefebvre, Phys. Rev. A **48**, 3845 (1993); **48**, 2855 (1993).

[18] R. Lefebvre and O. Atabek, Int. J. Quantum Chem. (to be published).

[19] A. Keller, Phys. Rev. A **52**, 1450 (1995).

[20] H. D. Feit, J. A. Fleck, and A. Steiger, J. Comput. Phys. **47**, 417 (1982).

[21] U. Fano, Phys. Rev. **124**, 1866 (1961).